Hindawi
Journal of Chemistry
Volume 2019, Article ID 2634398, 11 pages
https://doi.org/10.1155/2019/2634398

Research Article

SiO_2/TiO_2 Composite Coating on Light Substrates for Photocatalytic Decontamination of Water

Hana Bíbová,[1,2] Lenka Hykrdová,[1] Hiep Hoang,[3] Milan Eliáš,[1,2] and Jaromír Jirkovský[1]

[1]*Department of Electrochemical Materials, J. Heyrovsky Institute of Physical Chemistry of the CAS, v.v.i., 182 23 Prague 8, Czech Republic*
[2]*Faculty of Science, Charles University in Prague, 128 43 Prague 2, Czech Republic*
[3]*Vietnam National University of Agriculture, Gia Lam, Hanoi, Vietnam*

Correspondence should be addressed to Lenka Hykrdová; lenka.hykrdova@jh-inst.cas.cz and Hiep Hoang; hoanghiep@vnua.edu.vn

Received 15 March 2019; Revised 17 June 2019; Accepted 30 July 2019; Published 22 September 2019

Guest Editor: Ajit Kumar Sharma

In this study, we describe synthesis and characterization of a floating photocatalyst for water treatment consisting of a light substrate coated by SiO_2/TiO_2 composite. Three supports of natural origin were used: natural cork, expanded clay (Liapor), and volcanic porous glass (Sorbix). The photoactivity of the coated supports was tested in a laboratory photoreactor, with Liapor being the most photoactive support with good mechanical stability. The corresponding rate constant for the degradation of a model pollutant, 4-chlorophenol, was $7.8 \times 10^{-5}\ s^{-1}$. Detail characterization of the coated Liapor was obtained by XRF, SEM/EDX, and UV-Vis diffuse reflectance spectroscopy, and surface area measurements. Outdoor experiments were carried out with calcined Liapor and oxalic acid or methylene blue under sunlight on pilot reactors in the Czech Republic and Vietnam. We demonstrated satisfactory photocatalytic activity, long-term stability, and reusability of the new floating photocatalyst. The photoefficiency to mineralize oxalic acid in water under sunlight was estimated as 6.7% under the applied conditions.

1. Introduction

Procedures for contaminated water treatment are still being developed and optimized. Methods using heterogeneous photocatalysis by TiO_2 represent environmental friendly and economical processes that have been investigated for several decades [1]. They are based on the formation of pairs of charge carriers, electron and hole ($e^- + h^+$), in a semiconductor particle upon interaction with photons of sufficient energy (equation (1) [2]). Hydroxyl groups bound on the semiconductor surface are oxidized by migrating holes to hydroxyl radicals (·OH), oxidizing species powerful to accomplish total mineralization of organic compounds and even of microbes. In the presence of oxygen, electrons are consumed under the formation of superoxide radical anions ($\cdot O_2^-$).

$$TiO_2\left(e^- + h^+\right) \xrightarrow{O_2, H_2O} \cdot O_2^- + \cdot OH \quad (1)$$

Recently, floating photocatalysts have been increasingly studied due to their advantages, such as easy recovery after the treatment and wide variability of buoyant substrates. Photocatalytic layers were immobilized on various supports, such as graphite [3, 4], perlite [5, 6], vermiculite [7], diatomite powder [8, 9], light-expanded clay aggregate [10, 11], fly ash cenospheres [12–14], palm trunk [15], silica gel beads [16], and others. Besides TiO_2, other metal oxides deposited on a surface were used (e.g., $BiVO_4$ [14]).

Photocatalytic efficiency of the materials is often tested by means of a model compound degradation. Halogenated hydrocarbons are stable compounds commonly found as water pollutants due to their wide industrial use. They often show low biodegradability and photodegradability. That is why their representatives, such as 4-chlorophenol (4-CP), are selected as model compounds in photocatalytic studies [17–19]. The proposed mechanism of 4-CP degradation initiated by OH radical attack includes reaction pathways

leading both to the formation of hydroxylated benzene derivatives [20] and to the direct opening of aromatic ring [21].

Oxalic acid (OA) represents another model compound, suitable especially for larger scales and pilot experiments. Its oxidation by hydroxyl radical results directly in the formation of carbon dioxide and hydrogen peroxide (equation (2)) [22]. As a model reactant, OA was used in several studies [22–25].

$$\begin{aligned} HC_2O_4^- + \cdot OH &\longrightarrow OH^- + \cdot COOH + CO_2 \\ \cdot COOH + O_2 &\longrightarrow \cdot HO_2 + CO_2 \\ \cdot HO_2 + \cdot HO_2 &\longrightarrow H_2O_2 + O_2 \end{aligned} \quad (2)$$

The aim of the presented manuscript is to characterize low-density materials applicable as floating substrates for photocatalytic layers. The required properties of such light supports should include availability, stability, and environmental friendliness. Three different types of supports were selected and used: cork, Liapor, and Sorbix. Photocatalytic efficiency of the supports with immobilized layer of SiO_2/TiO_2 composite was tested both under the laboratory and outdoor conditions, with the use of 4-CP and OA as model pollutants. We accomplished our study by evaluating the photocatalyst performance in a pilot solar reactor.

2. Materials and Methods

4-Chlorophenol (4-CP) (Acros Organics, 99%) was used as a model pollutant in the laboratory-scale experiments. Its concentration was determined by HPLC (Agilent Technology 1200 Series; detection wavelength 254 nm, mobile phase 60 : 40 water/methanol, flow rate 1 mL/min, injection volume 20 μL, column LiChroCART® 125-4 LiChrosphere 100 RP-18 (5 μm)). Prior to injection, the samples were filtered with 0.45 μm HA filter (Millipore). UV-Vis spectra of the irradiated solutions of 4-CP were measured without filtration by spectrophotometer UV/Vis/NIR Lambda 19 (PerkinElmer).

Oxalic acid (g.r., Lachner, 99.6%) was used for the outdoor experiments. Its concentration was determined by manganometric titration with $KMnO_4$ (Fluka, ≥99.0% p.a.; H_2SO_4 was obtained from Lachner, ≥95% p.a.):

$$5H_2C_2O_4 + 2KMnO_4 + 3H_2SO_4 \longrightarrow 2MnSO_4 + K_2SO_4 + 10CO_2 + 8H_2O \quad (3)$$

Total organic carbon (TOC) was determined by TOC-Vwp Analyzer (Shimadzu). Prior to injection, the samples were filtered with 0.45 μm HA filter (Millipore).

Methylene blue (MB) (Sigma-Aldrich, 82%) was used as a model compound for the outdoor experiments in Vietnam. Its concentration was measured spectrophotometrically at 665 nm by Spectro UV-2550 (Labomed, Inc.).

Water glass (30% SiO_2, Vodní sklo, a.s.) and TiO_2 P25 (Evonik) were used for the coating of tested floating substrates (experiments in the Czech Republic).

The surface structure and morphology of Liapor and the applied layers were obtained by scanning electron microscopy coupled with energy dispersive X-ray (SEM/EDX) spectroscopy. SEM Philips XL 30 CP microscope equipped with EDX, Robinson, SE (secondary electron), and BSE (back-scattered electron) detectors were used. Composition of Liapor was measured by X-ray fluorescence (XRF) spectroscopy. The XRF elementary analysis was performed by 4 kW wavelength dispersive X-ray fluorescence spectrometer S4 Pioneer (Bruker AXS) equipped with a rhenium tube operated at 20–60 kV. The samples were prepared and analyzed by the GEO-QUANT method.

Diffuse reflectance spectrum of the SiO_2/TiO_2 composite layer was measured after the deposition of layers (0.5 mL of the solution was spread on the microscopic glass plate; the procedure and concentration of solutions were otherwise kept same as in the case of the coating of supports) by spectrophotometer UV/Vis/NIR Lambda 19 (PerkinElmer) equipped with the integration sphere. The detail procedure of data evaluation is described by Kočí et al. [26].

The BET specific surface area of Liapor and the applied layers was determined from the adsorption isotherms of N_2 at the boiling point of liquid nitrogen using a Micromeritics ASAP 2010 apparatus [27].

Liapor used for the outdoor experiments in Vietnam was coated by the commercially available suspension of photoactive TiO_2 Protectam FN2 according to the procedure recommended by the manufacturer (Advanced Materials-JTJ, Czech Republic). Protectam FN2 is protected by U.S. patent no. 8,647,565 (2009) and consists of about 74% of Aeroxide TiO_2 P25, the remaining part being an inorganic binder.

2.1. Floating Support. In this study, three types of substrates were selected that meet the following criteria: density lower than 1 kg·dm^{-3}, large surface area, low cost, easy accessibility, and environmental friendliness (as itself and with regard to possible degradation products) (Figure 1).

As the widely available organic material, raw cork (Korek Jelínek, spol. s.r.o.) was chosen. Inorganic support was represented by expanded volcanic glass perlit "Sorbix" (WB 0/3, Imerys) and expanded clay Liapor (Lias Vintířov). Density and grain size of chosen supports are listed in Table 1.

2.2. Preparation of Coated Floating Substrates. The preparation of the photoactive layers is based on the synthesis of SiO_2/TiO_2 composite described in the utility model [28], modified for the deposition on the studied supports. The synthesis employs general amphoteric properties of solid oxide materials when zero points of charge (pH_{zpc}) of TiO_2 and SiO_2 are different. At the appropriate pH value, TiO_2 particles are dominantly protonated while the particles of SiO_2 are negatively charged. As a result, spontaneous association among them occurs. It was found that colloidal suspensions of such composite are stable in a long-term period.

The coating procedure consisted of the following steps:

1st layer (water glass): cleaned (washed and dried under room temperature) substrates were dipped in the

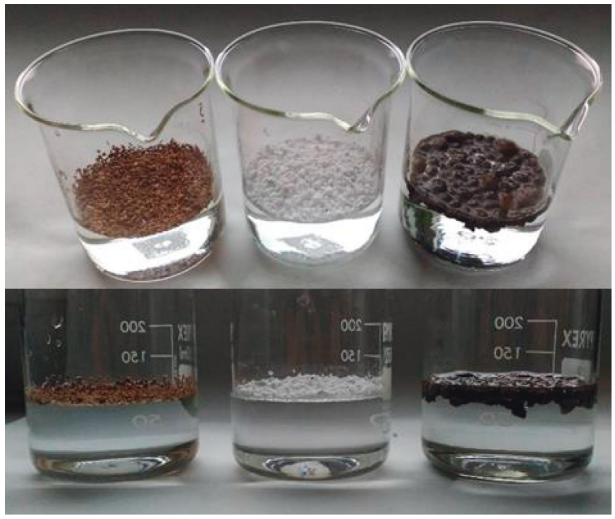

Figure 1: Floating supports (from the left cork, Sorbix, and Liapor) and demonstration of their stability on water surface.

Table 1: Properties of the floating substrates.

	Cork	Sorbix	Liapor
Density (kg·dm^{-3})	0.15–0.350	0.070	0.25–0.9
Grain size (mm)	0.5–3	<0.125	4–8

suspension of water glass (2 wt.% SiO_2) for 2 hours and then dried at 80°C. This step was performed in order to improve adhesion of the photocatalyst on the support surface.

2nd and 3rd layers (photocatalyst): support with the dried water glass layer was dipped in the suspension of 5 wt.% TiO_2 and 5.99 wt.% SiO_2 for 2 hours and then dried at 80°C.

Liapor samples for the outdoor experiments were further calcined at 250°C for 1 hour (temperature gradient 1°C/min).

The mechanical stability of the deposited layers was tested after washing (5 g) in demineralized water (0.1 dm^3) for 6 hours under stirring, followed by drying at room temperature.

2.3. Photoreactors and the Operating Conditions. Photocatalytic experiments were carried out in the photoreactors of our own design and construction (Figures 2(a) and 2(b)). The laboratory photoreactor (Figure 2(a)) enables to perform series of experiments under the identical conditions, thus reducing random effects. The bottom of the device consists of 6 or 15 magnetic stirrers (Variomag Telesystem) with a cut-out slab to keep the beakers with the tested solutions in constant positions. In the upper part, UV fluorescent lamps are installed that can be switched on/off separately. The inner walls of the photoreactor are covered by the brushed aluminum foil to maximize light reflection and ensure homogeneous irradiation. For the purpose of our study, the photoreactor was equipped with 10 fluorescent black lamps (λ_{max} = 365 nm, 8 watt, Sylvania), and the flux density at the probe level was 6.24 mW·cm^{-2} measured by UVA probe (ILT 1400-A Photometer, probe UVa #28949).

For the outdoor experiments, solar reactors of a larger scale were used (Figure 2(b)). In the 40 dm^3 plastic basin, the tested solution (25 dm^3) is pumped and circulates through the integrated jet system that causes regular rotation and watering of the floating photocatalyst. The solar reactors were covered by UVA transparent glass sheets ($A_{(300nm)} \leq 0.1$) to prevent evaporation of the tested solution. The weather conditions were monitored by an integrated sensor suite (ISS), the measured data sent to ForVantage Pro2 Plus™ console, and evaluated by WeatherLink software.

During the outdoor experiments in Vietnam, the intensity of the incident sunlight was monitored continuously by quantum meter (Apogee Instruments, Inc.).

The course of photocatalytic degradation of the model compound was formally described by the first-order kinetics. The corresponding rate constants were calculated by a nonlinear curve fitting procedure using the relation $c = c_0 e^{(-kt)}$, where c, t, and k represent concentration of 4-CP, time of irradiation, and rate constant, respectively.

3. Results and Discussion

3.1. Comparison of the Supports. The photoactivity of the supports was monitored by means of 4-CP degradation. Determination of photoactivity of the noncoated substrates was performed with 4-CP (2×10^{-4} mol·dm^{-3}, 0.1 dm^3) in the laboratory photoreactor (Figure 2(a)). In the case of Sorbix and Liapor, concentration of 4-CP remains constant during the whole irradiation time, that is, no measurable photoactivity of the floating substrates was found for at least 6 hours under stirring. Cork, on the other hand, releases a small amount of organic matter upon the contact with water. This phenomenon complicates determination of 4-CP concentration due to the high background response detected by UV-Vis spectroscopy and TOC and will be discussed further.

3.2. Photoactivity and Mechanical Stability of the Deposited Layers. The kinetics of 4-CP degradation was followed both by HPLC (Figures 3–5) and by the measurement of the relative change of TOC. Although the former value represents direct decrease of 4-CP concentration resulting from hydroxyl radical attack, the latter reflects mineralization to carbon dioxide that proceeds, due to complex degradation mechanism via various intermediates, much slower.

The course of photocatalytic degradation of 4-CP with coated Sorbix and Liapor follows formally the first-order kinetics (Figures 4 and 5). The values of corresponding rate constants and relative changes of TOC are summarized in Table 2.

In the case of using Sorbix as the floating substrate, the deposition of a stable layer is difficult because of the high hydrophobicity of the support. Low wettability of the prepared floating photocatalyst is thus associated with its low photoactivity (Table 2). At a stirring rate of 200 rpm, negligible degradation of 4-CP is observed and even 500 rpm is not

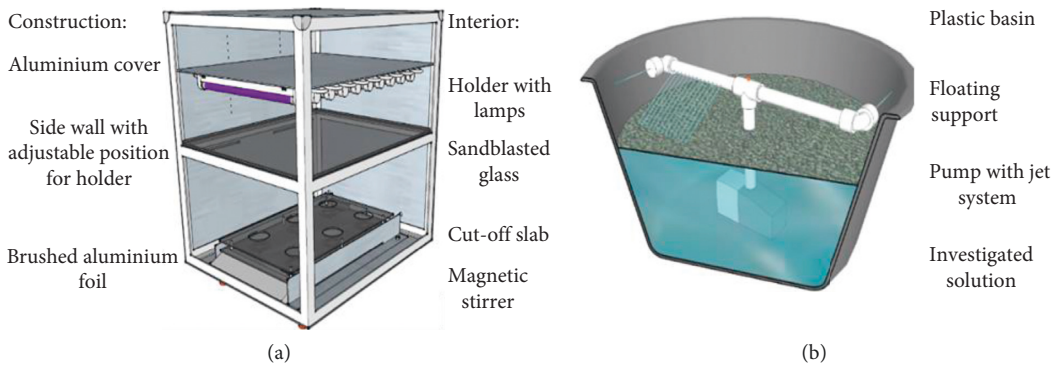

Figure 2: Photoreactors of our own design and construction. (a) Laboratory photoreactor. (b) Outdoor photoreactor.

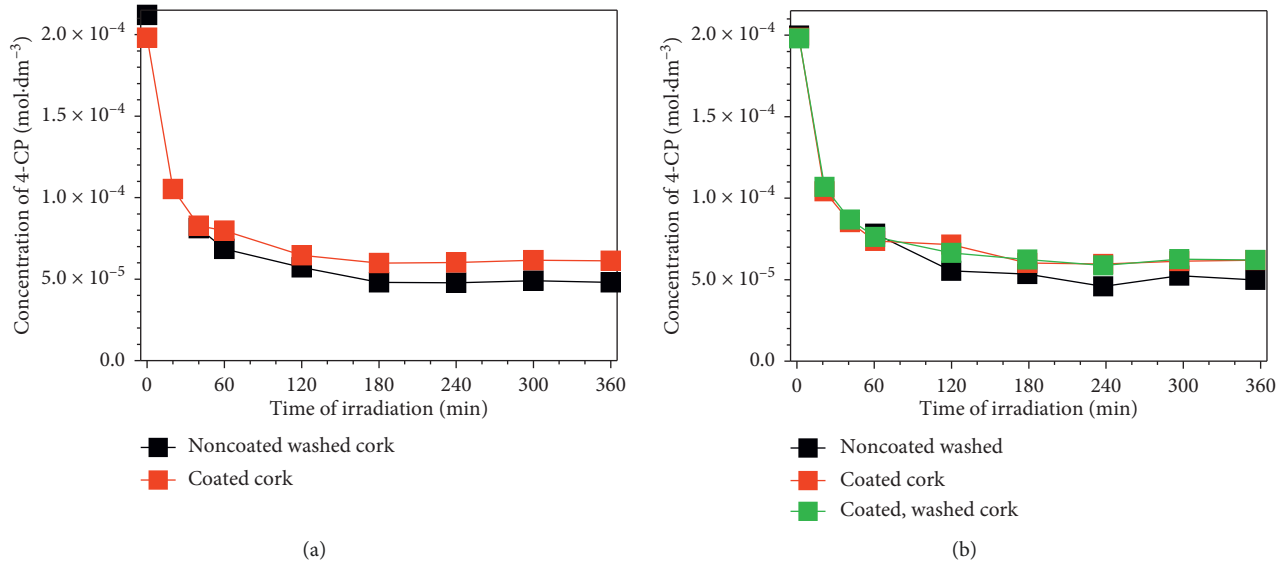

Figure 3: (a) Blank—sorption of 4-CP on Noncoated washed cork and coated cork. (b) Photocatalytic degradation of 4-CP (in laboratory photoreactor at a stirring rate of 500 rpm) using noncoated washed, coated, and coated, washed cork.

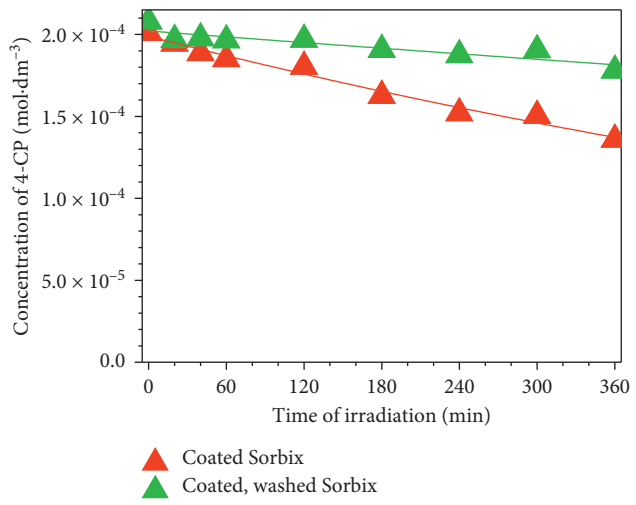

Figure 4: Photocatalytic degradation of 4-CP (in laboratory photoreactor at a stirring rate of 500 rpm) using coated Sorbix and coated, washed Sorbix.

sufficient to ensure satisfactory contact with the solution as after 6 hours of the irradiation; the concentration of 4-CP decreased only to 70% of its original value. The mechanical stability of the deposited layer is not satisfactory enough, since by washing, the degradation rate is reduced to one-third and a similar effect is observed in the case of TOC values (Table 2).

The physicochemical properties of Liapor enabled the preparation of a uniform stable layer according to the described procedure (90% of a particle volume was submersed in SiO_2 or SiO_2/TiO_2 aqueous suspensions). The surface of coated Liapor grains is sufficiently wetted during irradiation, and further increase of stirring rate does not alter the course of 4-CP degradation. Neither the adsorption of 4-CP on Liapor particles (both noncoated and coated) nor any other effects that could affect photocatalytic process were observed under the applied laboratory conditions.

The results of 4-CP degradation with coated Liapor are summarized in Table 2. Within 6 hours of the irradiation, concentration of 4-CP decreased approximately to 10% of its original value ($k = 7.80 \times 10^{-5}\ s^{-1}$). Washing has not changed

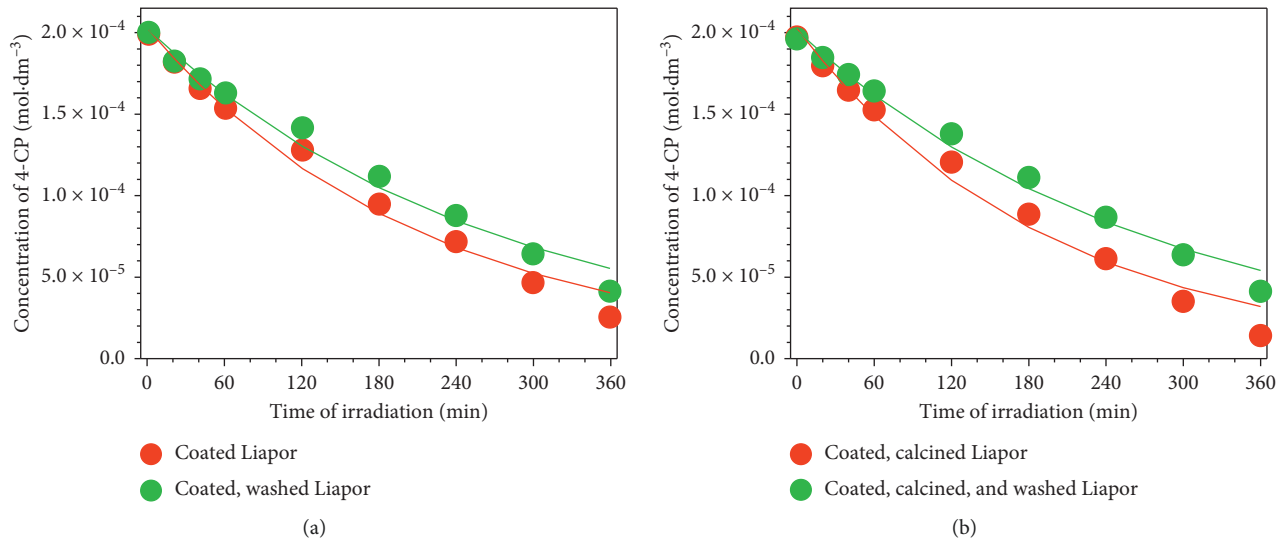

Figure 5: Photocatalytic degradation of 4-CP (in laboratory photoreactor at a stirring rate of 500 rpm) using (a) nonwashed and washed Liapor. (b) Calcined, and calcined, washed Liapor.

Table 2: Rate constants of 4-CP photocatalytic degradation and relative change of TOC after 6 hours of irradiation.

	Material	Rate constant (10^{-5} s^{-1})	TOC: relative change (%)
Sc	Sorbix: coated	1.72	76.3
Scw	Sorbix: coated and washed	0.50	89.1
Lc	Liapor: coated	7.80	27.0
Lcw	Liapor: coated and washed	6.22	40.1
Lcc	Liapor: coated and calcined	8.53	15.0
Lccw	Liapor: coated, calcined, and washed	6.08	37.2

the photoperformance of coated Liapor markedly (Figure 5(a) and Table 2).

Calcination of coated Liapor at 250°C leads to an increase of 4-CP degradation rate (8.53×10^{-5} s^{-1}) (Figure 5(b)). After washing, almost the same photoactivity of calcined Liapor and Liapor without the heat treatment is observed (6.08×10^{-5} s^{-1}). From the comparison of the data in Table 2, it can be concluded that Liapor represents the most appropriate floating substrate for the photocatalyst deposition.

Cork used as a support for the photocatalyst layer shows completely different physicochemical properties. Besides the aforementioned release of an organic matter, marked sorption effects occur when 4-CP is exposed to this floating substrate. Blank experiments without irradiation demonstrate significant adsorption of 4-CP on both noncoated and coated cork (Figure 3(a)). According to the experimental data, sorption processes play dominant role and photocatalytic degradation represents only a minor part under the applied experimental conditions, both before and after washing of the cork substrate (Figure 3(b)). Concentration decrease of 4-CP could not be approximated by the first-order kinetics.

3.3. Characterization of Liapor and the Deposited Layers. Liapor with deposited photocatalyst layer has been further studied in detail. The results of elemental analyses (XRF and EDS) show that this expanded clay consists of silicone oxide as the main component (41.02%, Table 3), and of aluminum and iron oxides as less abundant components. Titanium dioxide represents approximately 3% of the total oxide content.

Figure 6 shows SEM images of Liapor sample before the deposition of the photoactive layer. Original Liapor has a heterogeneous surface structure (Figure 6(a)). After water glass deposition, fine cracks typical of silicate layer appear on the surface (Figure 6(b)). The coated layer is thin as evidenced by EDS analysis that provides a similar elemental composition for both uncoated and coated samples (Figure 7(a) and Table 4).

Changes of Liapor surface structure due to the particular steps of the photoactive layer preparation, that is, coating and drying (Figure 8(a)), calcination (Figure 8(b)), and washing (Figure 8(c)) were also followed by SEM technique. Observed smooth layer of the photocatalyst copies depressions and protrusions of the support surface. Formed polygons are separated by numerous cracks. Surface mapping scans of samples show that the polygons consist of the deposited photocatalyst with Si, O, and Ti as the main atomic components (Figure 7(b), Table 4) while in the cracks, the original support surface is observed. The composite layers coated on Liapor substrate show high mechanical stability.

The value of bandgap energy was calculated from UV-Vis diffuse reflectance spectrum of the SiO_2/TiO_2 composite layers deposited on a quartz glass. Original coordinates of

Table 3: XRF analysis of Liapor.

Formula	SiO_2	Al_2O_3	Fe_2O_3	TiO_2	CaO	K_2O	MgO	Others
Concentration (%)	41.02	25.67	12.16	3.334	3.079	2.592	2.072	<0.5

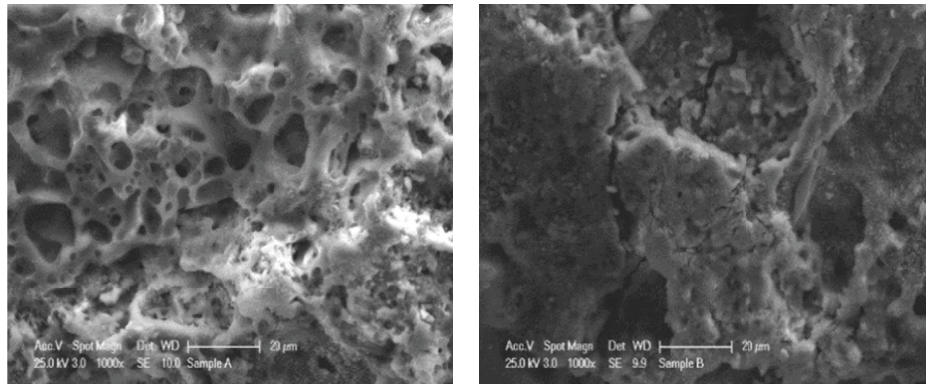

(a) (b)

Figure 6: SEM images of Liapor. (a) Liapor before coating. (b) Liapor with the first layer of SiO_2.

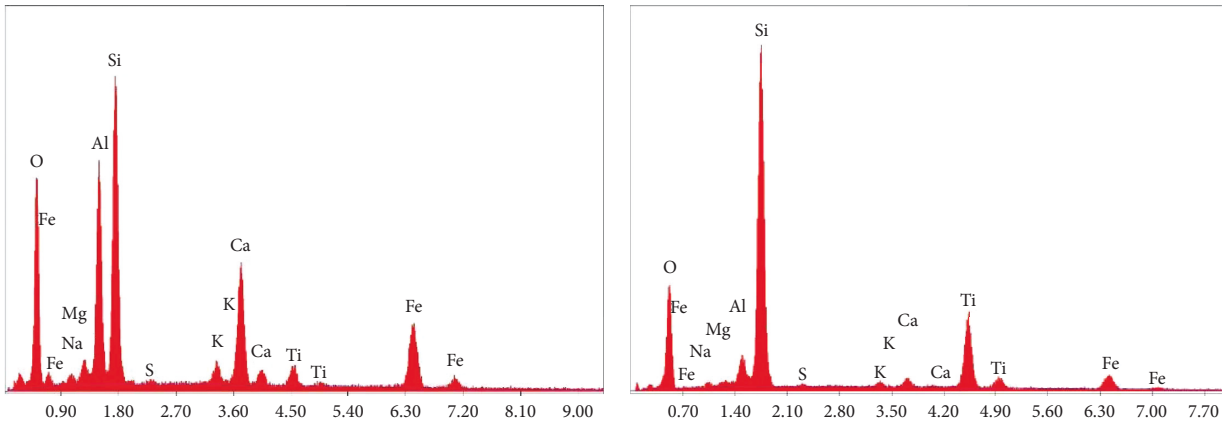

(a) (b)

Figure 7: EDS analyses of Liapor. (a) Liapor with the SiO_2 layer. (b) Liapor with the first layer of SiO_2 and two composite layers.

Table 4: EDS analysis of Liapor.

Element (wt.%)	Liapor	SiO_2 layer	Composite
O K	41.59	41.59	43.27
Na K	1.14	1.34	1.22
Mg K	2.14	2.08	0.97
Al K	15.13	13.81	3.56
Si K	20.20	19.95	32.54
S K	0.26	0.27	0.34
K K	2.33	1.44	0.63
Ca K	5.41	7.97	1.10
Ti K	1.69	1.76	12.32
Fe K	10.11	9.80	4.04

the spectrum, that is, reflectance vs. wavelength, were transformed to Kubelka–Munk function (K) vs. photon energy (hv). Bandgap energy is usually estimated by extrapolation of the linear part of the dependence; however, we employed a more precise method based on fitting of the experimental dependences by Boltzmann symmetrical function using nonlinear regression [26]. Then, the calculated crossing point of the tangent line in the inflection point of the Boltzmann fit with its lower asymptote determines the bandgap energy as 3.04 eV (Figure 9).

The surface area of the support and deposited layers was investigated by the measurement of adsorption isotherms of N_2 at 77 K. While the surface area of Liapor is only 0.15 $m^2 \cdot g^{-1}$, a marked increase to 1.2 $m^2 \cdot g^{-1}$ is observed after the deposition of SiO_2. Finally, the composite layer shows the largest value, 4.3 $m^2 \cdot g^{-1}$. The observed trend suggests that the photocatalyst specific surface area is maintained during its application.

3.4. Outdoor Experiments. The aim of parallel outdoor experiments was to test the photocatalytic activity of coated Liapor under sunlight. The experiments were carried out in the solar reactor depicted in Figure 2(b). Oxalic acid

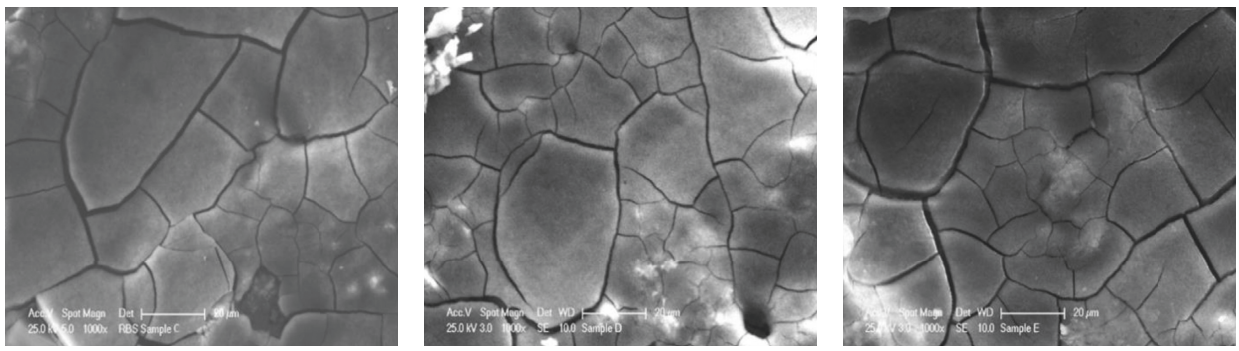

(a) (b) (c)

Figure 8: SEM images of Liapor coated with SiO_2 layer and two composite layers. (a) Dried at room temperature. (b) Calcined at 300°C. (c) Calcined at 300°C and washed for 6 hours.

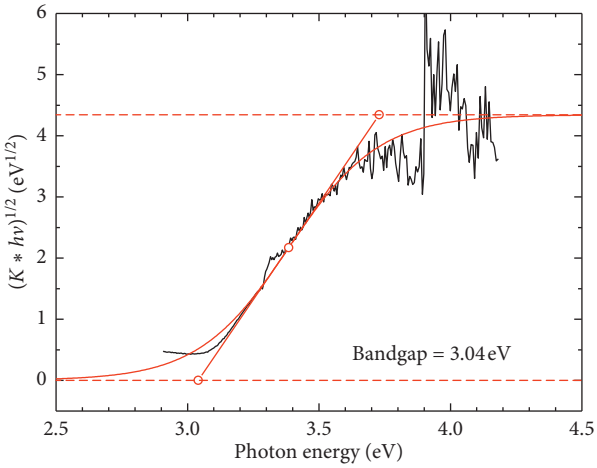

Figure 9: Transformed diffuse reflectance spectrum and determination of bandgap energy.

$(3.3 \times 10^{-3}$ mol·dm^{-3}, 25 dm^3) was chosen as a model compound due to its relative nontoxicity that allows its usage in large amounts. During the irradiation, temperature and UV index were monitored by the ISS probe. It was observed that direct photolysis of OA proceeded in parallel to its photocatalytic degradation, although at a much slower reaction rate. Therefore, the higher amount of the coated support, that is, 200 g (60% of water surface covered) was used in order to reduce the contribution of photolysis to the total photodecomposition.

Concentration changes of OA correlated with the solar radiation intensity (Figure 10(a)). At the end of the fourth day of the irradiation, OA was practically decomposed.

An appropriate initial concentration of OA for the experiments under the applied conditions (200 g of coated support, grain size 4–8 mm) was determined on the basis of another series of experiments (Figure 10(b)). While lower concentrations of OA would be decomposed too fast under sunny weather, high initial concentration would lead to unnecessarily long degradation time.

The size of Liapor grains (1–4 mm, 4–8 mm, and 8–16 mm) was another studied parameter (Figure 11(a)). Small grains (1–4 mm) show a large specific area; however, the smallest beads of expanded clay tend to immerse, thus resulting in the deceleration of the photocatalytic process. On the other hand, large coated grains (8–16 mm) flow easily on the water surface at the cost of a smaller specific area. Photocatalytic performance of both medium and large support grains is comparable.

The stability of the floating photocatalyst was tested by its repeated use under the otherwise same conditions (Figure 11(b)). No significant changes of the photocatalytic performance after one or two experimental cycles compared with the freshly prepared sample (200 g, grain size 4–8 mm) were observed. This fact signifies good stability and durability of the layer deposited on the Liapor substrate, a parameter important for the practical use of any photocatalyst.

3.5. Pilot Experiments in the Czech Republic and in Vietnam. To study the performance of the floating photocatalyst in a scale corresponding to its intended use, pilot experiments were performed. The solar reactor in the Czech Republic (Figure 12(a)) was designed to simulate the remediation of contaminated water in rural areas, for example, in the wells that were left after the bomb attacks during the Vietnam War. It consists of the round plastic pool ($V = 7$ m^3) equipped with a jet system, pump, and filter. The floating photocatalyst (coated, calcined Liapor) covered almost all water surface and was sprinkled by the jet system. As a model compound, oxalic acid (OA; 3.3×10^{-3} mol·dm^{-3}) was chosen, and instead of distilled water, ordinary tap water was used. This fact shows the importance of such type of experiments, as some cations present in water (Ca^{2+}, Mg^{2+}, and Fe^{3+}) tend to precipitate as insoluble oxalates. Therefore, these cations were initially removed from the solution by a sufficient excess of OA and subsequent filtration. It was found by EDX analysis that the precipitate contained predominantly Fe(III), indicating the presence of iron ions in the used tap water.

A typical course of the pilot solar experiment with OA in the presence of the floating photocatalyst is shown in Figure 12(b). Stepwise decrease of OA concentration, determined by both manganometric titration and TOC analysis, corresponds well to the day and night period. After

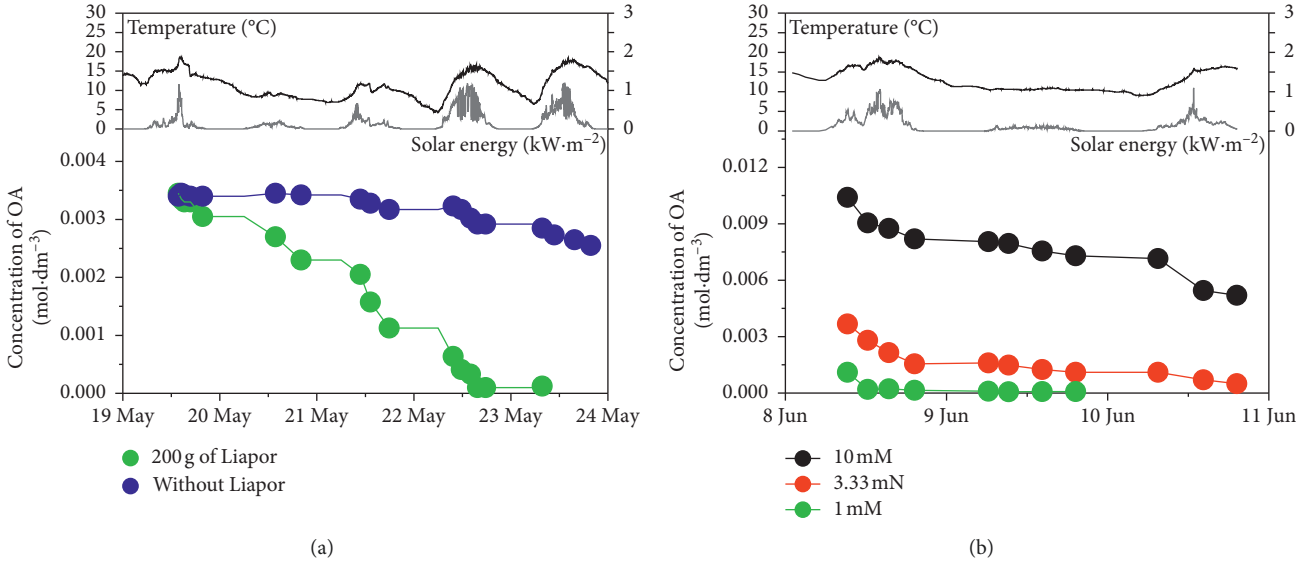

Figure 10: Photocatalytic degradation of OA. (a) Without (photolysis) and with coated, calcined Liapor. (b) Influence of OA concentration with coated, calcined Liapor, grain size 4–8 mm.

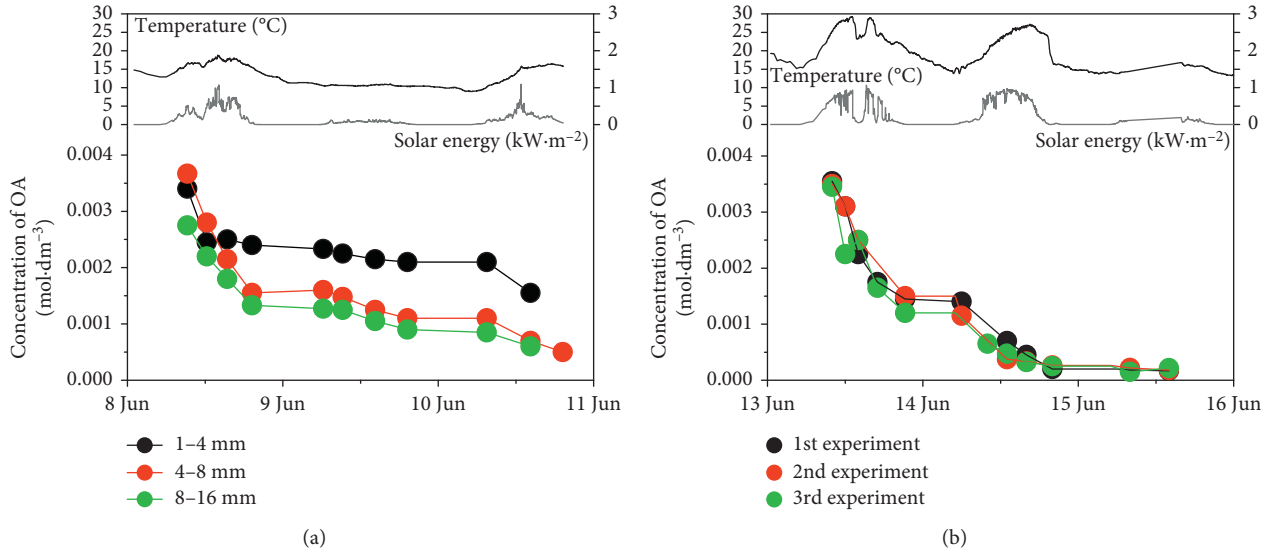

Figure 11: Photocatalytic degradation of OA with coated, calcined Liapor. (a) Different grain sizes (1–4 mm, 4–8 mm, and 8–16 mm). (b) Used for the first, second, and third time.

four days of irradiation, no detectable amount of OA remained in the solution and TOC dropped to 11.9% of its original value.

Comparative solar experiments were carried out in Vietnam, employing a special set of batch photoreactors (Figure 13(a)). The device consists of six glass compartments (50 dm^3 each) equipped with aeration, stirring, and a system preventing evaporation. About 2 cm below the solution level, metal plates are placed to prevent immersion of the floating photocatalyst. A typical daily course of solar radiation intensity is shown in the inset of Figure 13(b).

The floating photocatalyst was prepared by coating an expanded clay (analogous to the Liapor) with commercially available TiO_2 suspension with inorganic additives (Protectam FN2). Two grain sizes of the floating support were tested (5 mm and 10 mm).

As a model compound, methylene blue (MB, 3.3×10^{-6} mol·dm^{-3}) was used. Two hours before exposing to solar radiation, the tested solution and floating photocatalyst were left in dark to equilibrate adsorption of MB on the photocatalyst surface. Besides adsorption of MB on the photocatalyst surface, no other interaction was observed. Figure 13(b) shows time dependence of MB concentration during 6 days of solar irradiation. The decrease reflects photocatalytic degradation, in contrast to the overnight periods and the blank experiment, during which MB

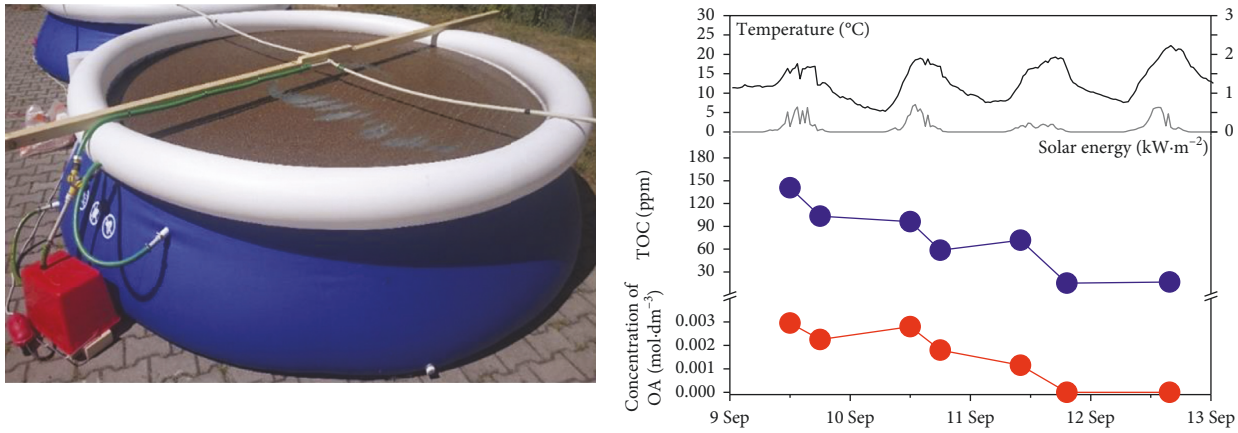

FIGURE 12: Pilot experiments in the Czech Republic. (a) Solar reactor with coated Liapor. (b) Photocatalytic degradation of OA during 4 days of solar irradiation.

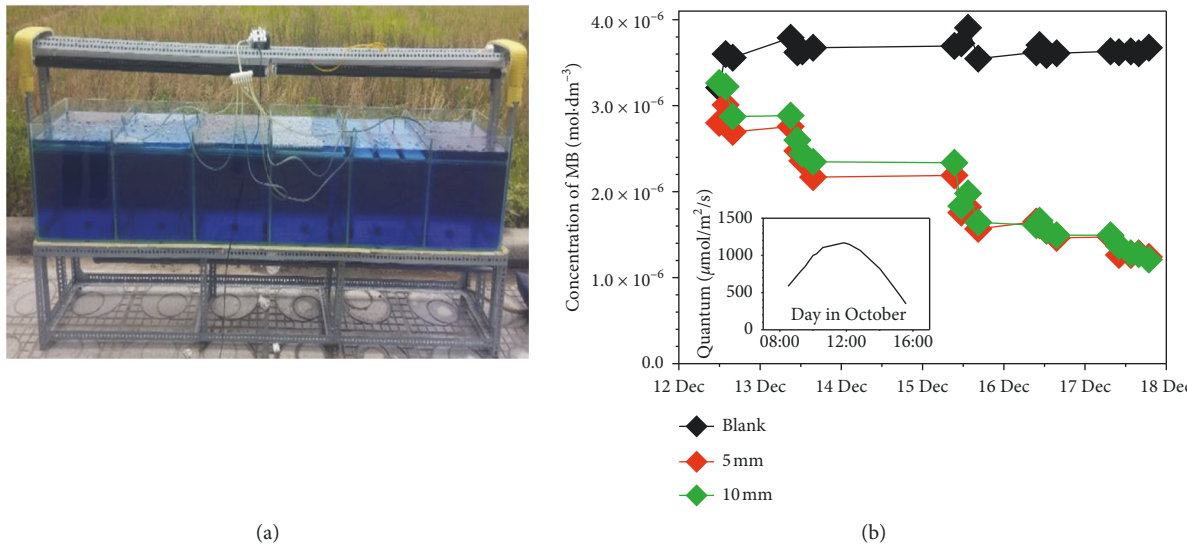

FIGURE 13: Pilot experiments in Vietnam. (a) Set of solar reactors with floating photocatalyst. (b) Photocatalytic degradation of MB during 6 days of solar irradiation.

concentration remained stable. The size of photocatalyst particles did not affect significantly the overall course of the photocatalytic degradation.

3.6. Estimation of the Photocatalyst Performance under Real Environmental Conditions. The intensity of solar radiation was measured and integrated during the whole period of outdoor experiments with oxalic acid. Thus, for example, in the case of the three-day experiment in the batch photoreactor (Figure 11(b)), the integrated solar radiation reached 13.38 kWh·m^{-2}, of which 5%, that is, 0.669 kWh·m^{-2}, represents UVA radiation available for TiO_2 photocatalysis. Considering, for simplification, UVA photons of a "middle" wavelength 380 nm, the value of 0.669 kWh·m^{-2} would correspond to 7.62 mol·m^{-2} of incident photons in three days (for detail calculation, see Supplementary Material (available here)). Applied to the parameters of our outdoor solar reactor and assuming the observed decrease of OA concentration, 0.082 moles of OA were mineralized by 1.23 moles of photons, which corresponds to a quantum efficiency 6.67%. This relatively high value might be partially attributed to a strong adsorption of OA on the photocatalyst surface that could cause its efficient oxidation by direct charge transfer mechanism.

The general capacity of the solar photocatalytic treatment of water can be approximately quantified. Provided that the mineralization of one organic carbon atom may require, on average, two subsequent photo-induced oxidative steps, then under the weather conditions typical of the central Vietnam (5.0 kWh·m^{-2}·day^{-1}, [29]), up to 0.095 moles of harmful organics can be mineralized by floating photocatalyst (e.g., Liapor with SiO_2/TiO_2 composite coating) covering area of 1 m^2 of contaminated water

in 1 day, using quantum efficiency calculated above. For a depth of 1 m and the corresponding volume of 1 m^3, the TOC content of contaminated water would thus be reduced by 1.14 ppm in one sunny day.

This is a promising result implying that solar photocatalysis can represent a method capable to decontaminate not only small water contents in the laboratory scale but also larger surface water amounts intended for cattle watering, fish breeding, etc. Hardly degradable toxic compounds presented in water at extremely low concentrations (such as 2,3,7,8-tetrachlorodioxin and DDT) can thus be successfully mineralized in order of days to weeks.

4. Conclusions

(i) Photocatalytic performance of SiO_2/TiO_2 composite deposited on three different floating substrates was tested by means of 4-CP photodegradation

(ii) Liapor with deposited SiO_2/TiO_2 composite showed high photoactivity and long-term durability

(iii) Coated Sorbix was less photoactive due to its high hydrophobicity

(iv) Cork was experimentally found as a less suitable support due to its strong adsorption properties and release of soluble organic matter

(v) SiO_2/TiO_2 composite layer on Liapor was characterized in detail, including atomic composition and surface microscopic images corresponding to each step of the deposition process

(vi) Pilot solar experiments demonstrated high efficiency, durability, and the ease of use of the new floating photocatalyst necessary for water decontamination

(vii) The efficiency of the new floating photocatalyst to mineralize organic matter in real contaminated surface water under sunlight was estimated

Data Availability

The data used to support the findings of this study are available from the corresponding authors upon request.

Conflicts of Interest

The authors declare that there are no conflicts of interest regarding the publication of this paper.

Acknowledgments

The authors acknowledge the assistance provided by the Research Infrastructure NanoEnviCz, supported by the Ministry of Education, Youth and Sports of the Czech Republic under Project no. LM2015073. This work was supported by the FIRST project, Subcomponent 1a—Foreign Talents STI Grants (no. 29/FIRST/1a/VNUA), the European Commission's Seventh Framework Programme (FP7) for Research and Technological Development (4G-PHOTOCAT, 309636), and Project AS CR (VAST-16-05). The authors would like to thank Dr. Jan Šubrt for SEM-EDS measurements and Dr. Michal Kolář for XRF analyses.

Supplementary Materials

Supplementary Material file contains a calculation procedure for determining the photocatalyst efficiency. (*Supplementary Materials*)

References

[1] S.-I. Kato and F. Mashio, "Titanium dioxide-photocatalyzed liquid phase oxidation of tetralin," *The Journal of the Society of Chemical Industry, Japan*, vol. 67, no. 8, pp. 1136–1140, 1964.

[2] O. Legrini, E. Oliveros, and A. M. Braun, "Photochemical processes for water treatment," *Chemical Reviews*, vol. 93, no. 2, pp. 671–698, 1993.

[3] X. Wang, X. Wang, J. Zhao et al., "An alternative to in situ photocatalytic degradation of microcystin-LR by worm-like N, P co-doped TiO_2/expanded graphite by carbon layer (NPT-EGC) floating composites," *Applied Catalysis B: Environmental*, vol. 206, pp. 479–489, 2017.

[4] A. Modestov, V. Glezer, I. Marjasin, and O. Lev, "Photocatalytic degradation of chlorinated phenoxyacetic acids by a new buoyant titania-exfoliated graphite composite photocatalyst," *The Journal of Physical Chemistry B*, vol. 101, no. 23, pp. 4623–4629, 1997.

[5] H. Joolaei, M. Vossoughi, A. Rashidi Mehr Abadi, and A. Heravi, "Removal of humic acid from aqueous solution using photocatalytic reaction on perlite granules covered by Nano TiO_2 particles," *Journal of Molecular Liquids*, vol. 242, pp. 357–363, 2017.

[6] Y. Shavisi, S. Sharifnia, S. N. Hosseini, and M. A. Khadivi, "Application of TiO_2/perlite photocatalysis for degradation of ammonia in wastewater," *Journal of Industrial and Engineering Chemistry*, vol. 20, no. 1, pp. 278–283, 2014.

[7] L. Jin and B. Dai, "TiO_2 activation using acid-treated vermiculite as a support: characteristics and photoreactivity," *Applied Surface Science*, vol. 258, no. 8, pp. 3386–3392, 2012.

[8] R. Cherrak, M. Hadjel, N. Benderdouche, S. Bellayer, and M. Traisnel, "Treatment of recalcitrant organic pollutants in water by heterogeneous catalysis using a mixed material (TiO_2-diatomite of Algeria)," *Desalination and Water Treatment*, vol. 57, no. 36, pp. 17139–17148, 2016.

[9] R. Zuo, G. Du, W. Zhang et al., "Photocatalytic degradation of methylene blue using TiO_2 impregnated diatomite," *Advances in Materials Sciences and Engineering*, vol. 2014, Article ID 170148, 7 pages, 2014.

[10] A. Mishra, A. Mehta, and S. Basu, "Clay supported TiO_2 nanoparticles for photocatalytic degradation of environmental pollutants: a review," *Journal of Environmental Chemical Engineering*, vol. 6, no. 5, pp. 6088–6107, 2018.

[11] Y. Shavisi, S. Sharifnia, M. Zendehzaban, M. L. Mirghavami, and S. Kakehazar, "Application of solar light for degradation of ammonia in petrochemical wastewater by a floating TiO_2/LECA photocatalyst," *Journal of Industrial and Engineering Chemistry*, vol. 20, no. 5, pp. 2806–2813, 2014.

[12] J. Song, X. Wang, Y. Bu et al., "Photocatalytic enhancement of floating photocatalyst: layer-by-layer hybrid carbonized chitosan and Fe-N- codoped TiO_2 on fly ash cenospheres," *Applied Surface Science*, vol. 391, pp. 236–250, 2017.

[13] J. Song, X. Wang, Y. Bu et al., "Preparation, characterization, and photocatalytic activity evaluation of Fe-N-codoped TiO_2/fly

ash cenospheres floating photocatalyst," *Environmental Science and Pollution Research*, vol. 23, no. 22, pp. 22793–22802, 2016.

[14] J. Zhang, H. Cui, B. Wang, C. Li, J. Zhai, and Q. Li, "Fly ash cenospheres supported visible-light-driven $BiVO_4$ photocatalyst: synthesis, characterization and photocatalytic application," *Chemical Engineering Journal*, vol. 223, pp. 737–746, 2013.

[15] M. Sboui, M. F. Nsib, A. Rayes, T. Ochiai, and A. Houas, "Application of solar light for photocatalytic degradation of Congo red by a floating salicylic acid-modified TiO_2/palm trunk photocatalyst," *Comptes Rendus Chimie*, vol. 20, no. 2, pp. 181–189, 2017.

[16] H. Taoda, "Development of TiO_2 photocatalysts suitable for practical use and their applications in environmental cleanup," *Research on Chemical Intermediates*, vol. 34, no. 4, pp. 417–426, 2008.

[17] M. Barbeni, E. Pramauro, E. Pelizzetti, E. Borgarello, M. Grätzel, and N. Serpone, "Photodegradation of 4-chlorophenol catalyzed by titanium dioxide particles," *Nouveau Journal de Chimie*, vol. 8, pp. 547–550, 1984.

[18] G. Shang, H. Fu, S. Yang, and T. Xu, "Mechanistic study of visible-light-induced photodegradation of 4-chlorophenol by $TiO_{2-x}N_x$with low nitrogen concentration," *International Journal of Photoenergy*, vol. 2012, Article ID 759306, 9 pages, 2012.

[19] B. Palanisamy, C. M. Babu, B. Sundaravel, S. Anandan, and V. Murugesan, "Visible-light active mesoporous ce incorporated TiO_2 for the degradation of 4-chlorophenol in aqueous solution," *Journal of Nanoscience and Nanotechnology*, vol. 13, no. 4, pp. 2572–2581, 2013.

[20] J. Theurich, M. Lindner, and D. W. Bahnemann, "Photocatalytic degradation of 4-chlorophenol in aerated aqueous titanium dioxide suspensions: a kinetic and mechanistic study," *Langmuir*, vol. 12, no. 26, pp. 6368–6376, 1996.

[21] V.-M. Guérin, R. Zouzelka, H. Bibova-Lipsova, J. Jirkovsky, J. Rathousky, and T. Pauporté, "Experimental and DFT study of the degradation of 4-chlorophenol on hierarchical micro-/nanostructured oxide films," *Applied Catalysis B: Environmental*, vol. 168-169, pp. 132–140, 2015.

[22] M. M. Kosanić, "Photocatalytic degradation of oxalic acid over TiO_2 power," *Journal of Photochemistry and Photobiology A: Chemistry*, vol. 119, no. 2, pp. 119–122, 1998.

[23] D. Tomova, V. Iliev, A. Eliyas, and S. Rakovsky, "Promoting the oxidative removal rate of oxalic acid on gold-doped CeO_2/TiO_2 photocatalysts under UV and visible light irradiation," *Separation and Purification Technology*, vol. 156, pp. 715–723, 2015.

[24] N. Barka, M. Abdennouri, A. Boussaoud et al., "Full factorial experimental design applied to oxalic acid photocatalytic degradation in TiO_2 aqueous suspension," *Arabian Journal of Chemistry*, vol. 7, no. 5, pp. 752–757, 2014.

[25] D. Santoro, F. Crapulli, A. Turolla, and M. Antonelli, "Detailed modeling of oxalic acid degradation by UV-TiO_2 nanoparticles: importance of light scattering and photoreactor scale-up," *Water Research*, vol. 121, pp. 361–373, 2017.

[26] K. Kočí, L. Obalová, L. Matějová et al., "Effect of TiO_2 particle size on the photocatalytic reduction of CO_2," *Applied Catalysis B: Environmental*, vol. 89, no. 3-4, pp. 494–502, 2009.

[27] T. Pauporte and J. Rathousky, "Growth mechanism and photocatalytic properties for dye degradation of hydrophobic mesoporous ZnO/SDS films prepared by electrodeposition, microporous and mesoporous," *Microporous and Mesoporous Materials*, vol. 117, no. 1-2, pp. 380–385, 2009.

[28] J. Jirkovský, F. Peterka, J. Šubrt, and M. Lambrecht, "Colloidal photo-catalytic composition," U. S. Patent US2013019684 5A1, 2013, https://patents.google.com/patent/US2013019 6845A1/es.

[29] https://www.pveducation.org/pvcdrom/properties-of-sunlight/average-solar-radiation.